

Coordination and local structure of Si and Al in silicate glasses: Si and Al K-edge XANES spectroscopy

DIEN LI,*¹ G. M. BANCROFT,¹ and M. E. FLEET²

¹Department of Chemistry, University of Western Ontario, London, Ontario N6A 5B7, Canada

²Department of Earth Sciences, University of Western Ontario, London, Ontario N6A 5B7, Canada

Abstract—Silicon K-edge XANES spectra of low-pressure glasses along the CaMgSi₂O₆ (Di)-NaAlSi₃O₈ (Ab) join and high-pressure Na₂Si₂O₅, Na₂Si₄O₉, and K₂Si₄O₉ glasses, and Al K-edge XANES spectra of high-pressure glasses along the NaAlSi₂O₆ (Jd)-NaAlSi₃O₈ (Ab) join are reported using synchrotron radiation. Ab₁₀₀ glass is very similar to albite in respect to the energy position and FWHM of the Si K-edge peak. Along the CaMgSi₂O₆ (Di)-NaAlSi₃O₈ (Ab) join, the Si K-edge peak shifts to lower energy and its FWHM increases dramatically with increase in Di content. These results indicate that the glasses become less polymerized and structural entities tend to become more complicated toward the Di end-member composition. The Di₁₀₀ glass contains Q⁰, Q¹, Q², Q³ and Q⁴ structural entities, although Q¹ (and possibly Q⁰ also) entities are predominant.

Aluminum K-edge XANES spectra of high-pressure glasses along the NaAlSi₂O₆ (Jd)-NaAlSi₃O₈ (Ab) join provide direct experimental evidence for the pressure-induced coordination change of Al from 4 to 6. Five- and six-coordinated Al (²⁷Al, ¹⁶⁷Al) appear in the Jd₆₀Ab₄₀ glass and become more prominent in the Jd₁₀₀ glass, indicating that the pressure required for the coordination change of Al in Jd₁₀₀ glass (*e.g.*, ~4 GPa) is lower than that in Ab₁₀₀ glass. The abundances of each of ²⁷Al and ¹⁶⁷Al in the Jd₁₀₀ glass are estimated to be about 6% of total Al. Silicon K-edge XANES spectra are also used to probe pressure-induced coordination change of Si in high-pressure glasses of composition Na₂Si₂O₅, Na₂Si₄O₉, and K₂Si₄O₉. Although the Si K-edge spectra provide no evidence for five-fold coordinated Si (²⁹Si) in these glasses, six-fold coordinated Si (¹⁶⁷Si) is present in Na₂Si₄O₉ and K₂Si₄O₉ composition glasses, confirming earlier ²⁹Si MAS NMR measurements. However, the abundance of ¹⁶⁷Si is higher in K₂Si₄O₉ glasses than in Na₂Si₄O₉ glasses, and increases with increasing pressure for glasses of the same chemical composition.

INTRODUCTION

SILICON IS four-fold coordinated (²⁹Si) with oxygen in silicates of the Earth's crust (*e.g.*, SMYTH and BISH, 1988), but becomes six-fold coordinated (¹⁶⁷Si) at high pressure. For example, silicon dioxide (SiO₂) has numerous polymorphic modifications with 4:2 coordinated structures (*e.g.*, quartz, cristobalite and tridymite), and occurs as stishovite with 6:3 coordinated structure at high temperature and pressures beyond about 9 GPa. Materials in the Earth's mantle are believed to be iron-bearing magnesium silicates with ²⁹Si structures dominant in the upper mantle and ¹⁶⁷Si structures predominant in the lower mantle (*e.g.*, ITO and TAKAHASHI, 1987; JEANLOZ, 1990; FINGER and HAZEN, 1991). Crystal-line SiP₂O₇ is one of several compounds in which Si occurs in octahedral coordination with oxygen at atmospheric pressure (*e.g.*, LIEBAU, 1985; FINGER and HAZEN, 1991).

Aluminum is either four- or six-fold coordinated (²⁷Al or ¹⁶⁷Al) with oxygen in most crystalline aluminosilicate minerals but it also occurs in five-fold coordination (²⁷Al) in andalusite (*e.g.*, SMYTH and BISH, 1988). However, both Al and Si are four-

fold coordinated with oxygen in silicate and aluminosilicate glasses at room temperature and pressure, because the octahedral coordination of Si and Al in glasses would force periodicity and disrupt the vitreous state (ZACHARIASEN, 1932). The only exceptions to date are that six-fold coordinated Si is evident in silicate-phosphate glasses with P₂O₅ above 32 mol% (DUPREE *et al.*, 1987; SEKIYA *et al.*, 1988; LI *et al.*, 1995c), and five-fold coordinated Si (²⁹Si) has been reported in K₂Si₄O₉ glass at atmospheric pressure (STEBBINS, 1991). Aluminum and Si have been reported in five- or six-fold coordination with oxygen in high-pressure silicate glasses and melts (*e.g.*, OHTANI *et al.*, 1985; STEBBINS, 1987; STEBBINS and McMILLAN, 1989; STEBBINS and SYKES, 1990; STOLPER and AHRENS, 1987; WILLIAMS and JEANLOZ, 1988; XUE *et al.*, 1989, 1991; LI *et al.*, 1994c), although the four-fold coordinated state dominates for both Al and Si in all of the vitreous materials investigated to date.

A knowledge of the structure of silicate melts and its relationship to their physical and chemical properties is necessary in order to understand magmatic processes. However, direct *in situ* spectroscopic study of silicate melt structure at both high temperature and high pressure is difficult experimentally, even though recent *in situ* Raman (HEMLEY *et al.*, 1986; MYSEN, 1990, 1995; MYSEN and

* Present address: National Institute of Materials and Chemical Research, Tsukuba, Ibaraki 305, Japan

FRANTZ, 1993, 1994; McMILLAN *et al.*, 1992; 1994) and MAS NMR studies (FARNAN and STEBBINS, 1990; POE *et al.*, 1993; STEBBINS, 1988a, 1988b) have provided important information on silicate melts at high temperature or at combined high temperature and pressure. It is generally assumed that the structure of a quenched glass represents that of the liquid at its glass transition temperature (*e.g.*, GIBBS and DIMARZIO, 1958), although some local structural changes may occur during quenching (McMILLAN *et al.*, 1992; MYSEN and FRANTZ, 1993).

The structure of silicate glasses has been extensively studied by X-ray diffraction (TAYLOR and BROWN, 1979), infrared (WONG and ANGELL, 1976) and Raman spectroscopy (McMILLAN, 1984a; McMILLAN and PRIOU, 1983; MYSEN, 1988), MAS NMR spectroscopy (KIRKPATRICK, 1988, STEBBINS, 1988b, STEBBINS and FARNAN, 1989), and metal K-edge X-ray absorption spectroscopy (GREAVES *et al.*, 1981; WAYCHUNAS *et al.*, 1988; JACKSON *et al.*, 1993; GALOISY and CALAS, 1994). The results indicate that the intermediate-range structure of silicate and aluminosilicate glasses may be described by a mixture of different structural units or entities of interconnected TO_4 tetrahedra (T = Si and Al) (MYSEN, 1988; McMILLAN, 1984a).

Aluminum K-edge X-ray absorption spectra of silicate glasses (McKEOWN *et al.*, 1985) and Si and O K-edge XANES spectra of densified vitreous silica (DAVOLI *et al.*, 1992) have been reported. In our previous papers, we reported Si K- and L-edge XANES spectra of silica polymorphs (LI *et al.*, 1994a), crystalline SiP_2O_7 (LI *et al.*, 1994b), silicate minerals (LI *et al.*, 1995a) and $\text{SiO}_2\text{-P}_2\text{O}_5$ and $\text{Na}_2\text{O-SiO}_2\text{-P}_2\text{O}_5$ glasses (LI *et al.*, 1995b, 1995c), and Al K-edge XANES spectra of aluminosilicate minerals (LI *et al.*, 1995d). The Si and Al K-edge XANES spectra have been used to distinguish different coordinations of Si (^{41}Si and ^{61}Si) and Al (^{41}Al , ^{51}Al and ^{61}Al) (LI *et al.*, 1994a, 1994b, 1995d). The Si K-edge shifts to higher energy with increase in polymerization of SiO_4 tetrahedra and to lower energy with the substitution of Al for Si in silicate minerals (LI *et al.*, 1995a). Silicon remains four-fold coordinated in $\text{SiO}_2\text{-P}_2\text{O}_5$ and $\text{Na}_2\text{O-SiO}_2\text{-P}_2\text{O}_5$ glasses with P_2O_5 below 32 mol%, but Na_2O depolymerizes and P_2O_5 copolymerizes these glasses (LI *et al.*, 1995b). However, ^{61}Si occurs in $\text{SiO}_2\text{-P}_2\text{O}_5$ and $\text{Na}_2\text{O-SiO}_2\text{-P}_2\text{O}_5$ glasses with P_2O_5 above 32 mol%; the proportion of ^{61}Si increases with increasing content of P_2O_5 , and is semi-quantitatively estimated by curve-fitting the Si K-edge spectra (LI *et al.*, 1995c).

In this paper, we report Si and Al K-edge XANES

spectra of $\text{CaMgSi}_2\text{O}_6\text{-NaAlSi}_3\text{O}_8$ glasses quenched at low pressure (1 bar), and $\text{NaAlSi}_2\text{O}_6\text{-NaAlSi}_3\text{O}_8$, $\text{Na}_2\text{Si}_2\text{O}_5$, $\text{Na}_2\text{Si}_4\text{O}_9$ and $\text{K}_2\text{Si}_4\text{O}_9$ glasses quenched at high pressure. We extend applications of Si and Al K-edge XANES spectroscopy at room temperature and pressure to investigate the polymerization of SiO_4 tetrahedra in room-pressure silicate glasses, and pressure-induced coordination changes of Si and Al in high-pressure silicate and aluminosilicate glasses. Preliminary results for the $\text{NaAlSi}_2\text{O}_6\text{-NaAlSi}_3\text{O}_8$ join are reported elsewhere (LI *et al.*, 1995e).

EXPERIMENTAL METHODS

Sample preparation

The $\text{CaMgSi}_2\text{O}_6\text{-NaAlSi}_3\text{O}_8$ glass samples were from the study of KEPPLER (1992). Mixtures of glassy powders of albite and diopside starting materials were melted in a platinum crucible using a room-pressure high-temperature gas mixing furnace. Experiments were performed in air, pure O_2 , or $\text{H}_2\text{-CO}_2$ mixtures. After usually 12–24 h at 1200–1500°C, samples were quenched by dropping the crucible into cold water. Other details on the sample preparation and composition of these glasses are given in KEPPLER (1992).

For study of glasses along the $\text{NaAlSi}_2\text{O}_6$ (Jd)- $\text{NaAlSi}_3\text{O}_8$ (Ab) join, the end-member compositions were prepared from stoichiometric proportions of Na_2CO_3 , Al_2O_3 and commercial "amorphous" SiO_2 , that were ground and mixed, contained in a platinum crucible with a closely fitted lid, and heated initially at 900°C for 1 day and finally at 1000°C for several hours. Intermediate starting compositions were prepared from mechanical mixtures of molar proportions of the end-members. High-pressure glasses were prepared using the 1000-t cubic anvil press at UWO. Samples were contained in BN crucibles, held at 4.4 GPa and 1575°C for 5 to 10 minutes, and quenched by switching off the power to the furnace (see LI *et al.*, 1995e for further details).

The high-pressure alkali silicate glasses were prepared using the MA6/8 superpress at the University of Alberta, Edmonton. Alkali silicate starting materials were prepared from carbonate-oxide mixtures. For the high-pressure experiments, samples were contained in a platinum capsule, and capsules were dried at 300°C for at least 1 hour before welding. Other experimental details are given in Table 1.

Si and Al K-edge XANES spectroscopy

Both Si and Al K-edge XANES spectra of glasses were collected on a double crystal monochromator (DCM) using synchrotron radiation. InSb (111) monochromator crystals were used for Si K-edge measurements, giving an energy resolution of 0.8 eV at 1840 eV (YANG *et al.*, 1992); and α -quartz (10 $\bar{1}$ 0) crystals were used for the Al K-edge measurements with an energy resolution of about 0.7 eV at 1560 eV. For both Si and Al K-edge measurements, very fine powder samples were spread uniformly on electric carbon tape supported on a stainless steel sample holder. The area covered by the sample was about 10 mm \times 10 mm and the sample thickness was reasonably constant for the measurement of each sample. Both Si and Al K-edge spectra were recorded by total electron yield (TEY) which measures the sample current from the escape of electrons of different energies from the surface

Table 1. Synthesis of $\text{Na}_2\text{Si}_2\text{O}_5$, $\text{Na}_2\text{Si}_4\text{O}_9$ and $\text{K}_2\text{Si}_4\text{O}_9$ glasses

Sample	Composition	Furnace	P (GPa)	T (°C)	Duration (min.)
1666	$\text{Na}_2\text{Si}_2\text{O}_5$	18M stepped graphite	8	1500	30
1665	$\text{Na}_2\text{Si}_2\text{O}_5$	18M stepped graphite	5	1500	30
1675*	$\text{Na}_2\text{Si}_2\text{O}_5$	18M stepped graphite	4	900	240
1709	$\text{Na}_2\text{Si}_4\text{O}_9$	14M LaCrO_3 High-T	12	1900	20
1685	$\text{Na}_2\text{Si}_4\text{O}_9$	18M stepped LaCrO_3	8	1900	20
1670	$\text{Na}_2\text{Si}_4\text{O}_9$	18M stepped LaCrO_3	6	1900	20
1673*	$\text{Na}_2\text{Si}_4\text{O}_9$	18M low-T stepped graphite	4	900	240
1676	$\text{K}_2\text{Si}_4\text{O}_9$	18M stepped LaCrO_3	6	1900	20
1682	$\text{K}_2\text{Si}_4\text{O}_9$	18M high-T stepped graphite	4	1900	20
1669*	$\text{K}_2\text{Si}_4\text{O}_9$	18M low-T stepped graphite	4	900	240

* #1675 is $\epsilon\text{-Na}_2\text{Si}_2\text{O}_5$ (FLEET and HENDERSON, 1995a); #1673 appears to be vitreous; #1669 is wadeite-structure $\text{K}_2\text{Si}_4\text{O}_9$ (SWANSON and PREWITT, 1983).

due to excitation by synchrotron X-radiation, and is proportional to the absorption coefficient (μ).

All samples were prepared in a similar manner to minimize the effect of sample thickness and particle size on the XANES features. Three measurements were made for each sample. The spectrum for each measurement was normalized by I/I_0 , where I is the intensity of TEY signal and I_0 is the intensity of photon flux. The raw spectrum for each sample investigated was averaged from three normalized measurements, and smoothed. A linear pre-edge background was removed from each spectrum. All Si K-edge XANES spectra were calibrated against the Si K-edge of α -quartz at 1846.8 eV, and all Al K-edge spectra were calibrated by the Al K-edge of Al foil at 1560.0 eV.

RESULTS AND DISCUSSION

Si K-edge XANES spectra of $\text{CaMgSi}_2\text{O}_6$ - $\text{NaAlSi}_3\text{O}_8$ glasses

Figure 1 shows the Si K-edge XANES spectra of a series of glasses along the $\text{CaMgSi}_2\text{O}_6$ (Di)- $\text{NaAlSi}_3\text{O}_8$ (Ab) join, as well as crystalline diopside and albite. The Si K-edge features of the end-member $\text{CaMgSi}_2\text{O}_6$ (Di_{100}) and $\text{NaAlSi}_3\text{O}_8$ (Ab_{100}) glasses and an intermediate composition ($\text{Ab}_{50}\text{Di}_{50}$) glass are expanded as dot, dash and solid lines, respectively, in the inset. The spectra of these Di-Ab glasses are generally similar. The Si K-edge peak, designated as $\text{C-}^{14}\text{Si}$, is prominent in the glass spectra, but the post-edge features are more-or-less smeared out compared with spectra for the corresponding minerals. This is anticipated from the disordered structure of glasses. The Si K-edge peak is assigned to transitions of Si 1s electrons to

the antibonding 3p-like t_2 states (Li *et al.*, 1994a). The energy position of the Si K-edge peak indicates that Si in the glasses is four-fold coordinated (Li *et al.*, 1994a). However, we note that the position of the Si K-edge peak of the glasses shifts to lower energy, and its full width at half maximum (FWHM) increases progressively, from Ab_{100} glass to $\text{Ab}_{50}\text{Di}_{50}$ and Di_{100} glasses.

Figure 2 shows the variations in energy position and FWHM of the Si K-edge peak with composition in this series of glasses. The open symbols are data for the glasses, and the filled symbols are data for crystalline diopside and albite. The Si K-edge peak shifts to lower energy by about 0.5 eV and its FWHM increases from about 2.5 to 4.1 eV with increase in molar proportion of Di component through the binary composition series. In addition, the energy position of the Si K-edge peak and its FWHM are very similar for both crystalline albite and Ab_{100} glass. However, the Si K-edge peak of Di_{100} glass shifts to much lower energy and its FWHM increases greatly compared with crystalline diopside.

The Si K-edge XANES spectra of silicate minerals demonstrated that the Si K-edge peak shifts to higher energy with increase in polymerization of SiO_4 tetrahedra and to lower energy with substitution of Al for Si (Li *et al.*, 1995a). Thus, the similarity in both Si K-edge peak position and FWHM for Ab_{100} glass and albite indicates that Ab_{100} glass has fully polymerized (Q^4) structural units, as in crystalline albite. However, the glasses along the

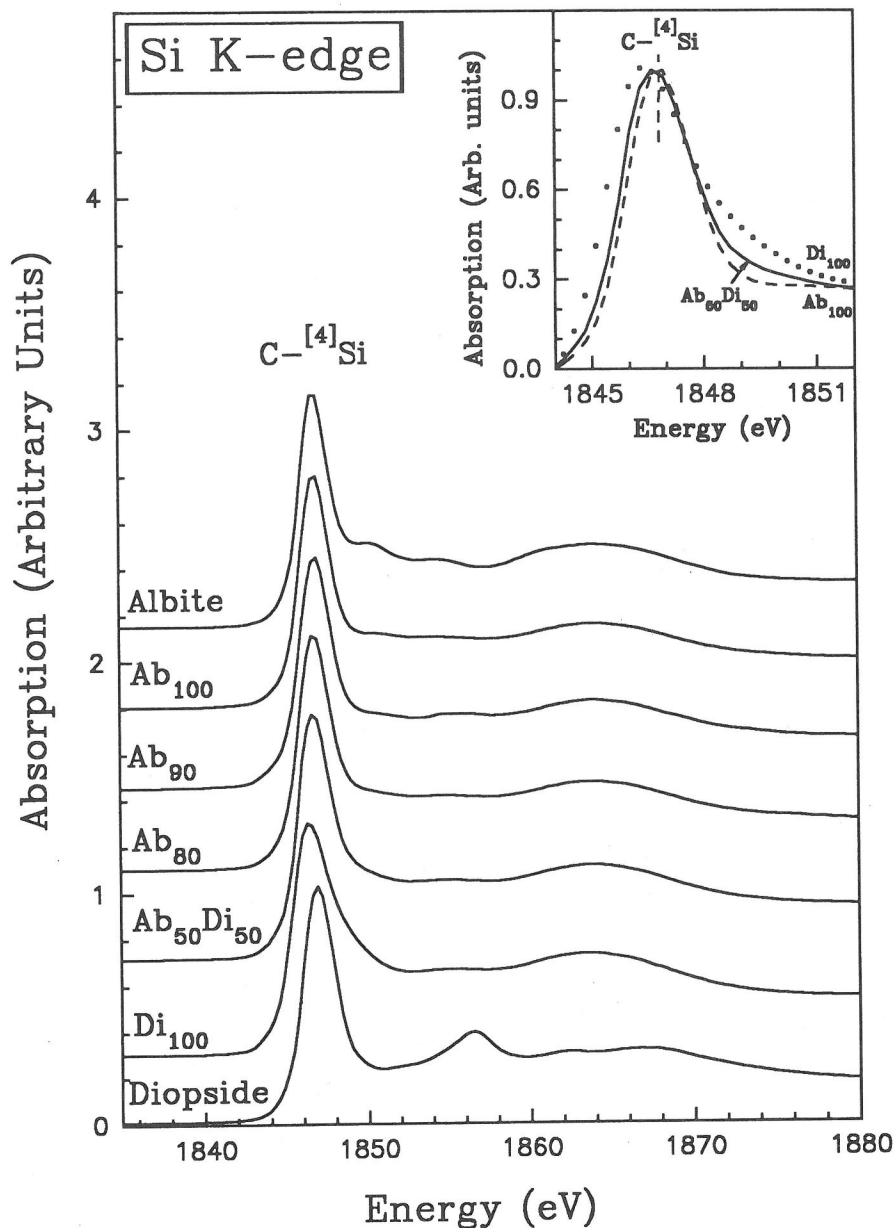


Fig. 1. Silicon K-edge XANES spectra of low-pressure glasses along the $\text{CaMgSi}_2\text{O}_6$ (Di)- $\text{NaAl-Si}_3\text{O}_8$ (Ab) join. The ^{41}Si K-edge features of Di_{100} , $\text{Ab}_{50}\text{Di}_{50}$ and Ab_{100} glasses are expanded in the inset as dot, solid and dash lines, respectively.

Ab-Di join become progressively less polymerized and the Si K-edge peak shifts to lower energy with increasing Di content, paralleling changes in the structure and Si K-edge XANES spectra of the corresponding crystalline minerals (Li *et al.*, 1994a). We have two interpretations for the progressive increase in the FWHM of the Si K-edge peak of glasses along the Di-Ab join. First, five-

and/or six-coordinated Si (^{5}Si , ^{6}Si) may occur in the glasses towards the Di end member, because a shoulder at about 1848.5 eV appears in the Si K-edge XANES spectra of $\text{Ab}_{50}\text{Di}_{50}$ glass and becomes more evident in the spectrum of Di_{100} glass (Li *et al.*, 1994a). However, we were not able to confirm this conclusion by ^{29}Si MAS NMR measurements because of the very small amount of

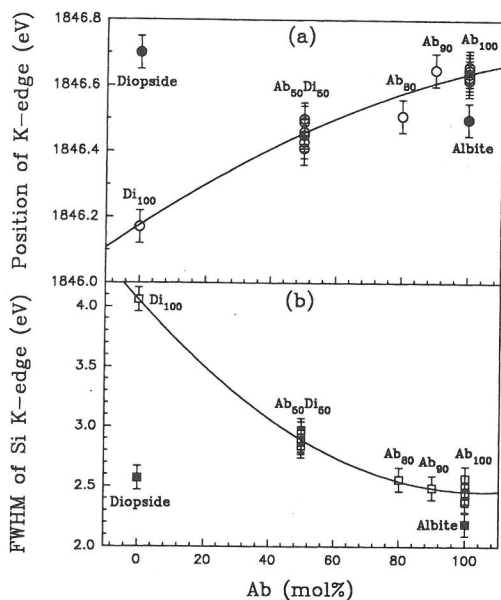


FIG. 2. Variations of energy position (a) of Si K-edge peak and its FWHM with the content of Ab in glasses (open symbols) along the Di-Ab join. The filled symbols represent data for crystalline albite and diopside. The Si K-edge peak shifts to lower energy, and its FWHM increases with decreasing content of Ab, from Ab_{100} to Di_{100} . Note that the structure of Di_{100} glass appears to be significantly different from that of crystalline diopside.

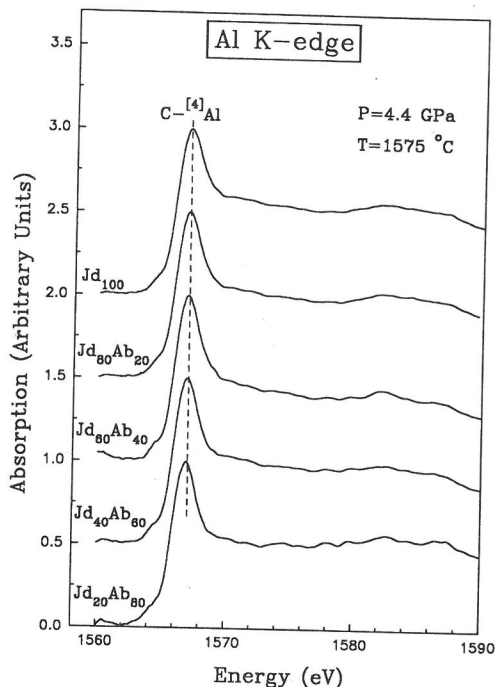


FIG. 3. Aluminum K-edge XANES spectra of high-pressure glasses along the $NaAlSi_2O_6$ (Jd)- $NaAlSi_3O_8$ (Ab) join. The prominent edge peak is attributed to $[4]Al$. A shoulder at about 1568.5 eV becomes more prominent with increasing content of Jd .

glass samples available for this study. Second, the most likely interpretation is that the intermediate-range structure in these glasses is complex, and becomes progressively more complicated toward the Di end-member composition. Di_{100} glass has an average of two nonbridging oxygens per tetrahedral cation. However, although individual peaks in the Si K-edge region are not resolved, as in corresponding ^{29}Si MAS NMR spectra (KIRKPATRICK *et al.*, 1986), the Di_{100} glass may contain local structural entities with different polymerization (Q^0 , Q^1 , Q^2 , Q^3 and Q^4). These results are in good agreement with ^{29}Si MAS NMR (MURDOCH *et al.*, 1985; KIRKPATRICK *et al.*, 1986) and Raman spectroscopy (MCMILLAN, 1984b).

Al K-edge XANES spectra of $NaAlSi_2O_6$ - $NaAlSi_3O_8$ glasses

Figure 3 shows the Al K-edge XANES spectra of high-pressure glasses along the $NaAlSi_2O_6$ (Jd)- $NaAlSi_3O_8$ (Ab) join. The Al K-edge spectra for these glasses of different composition are generally similar. The Al K-edge peak is prominent (shown normalized to one unit in intensity), and is assigned

to the transitions of Al 1s electrons to antibonding 3p-like t_2 states, by analogy with the Si K-edge peak, as in LI *et al.* (1995d). The energy position of the Al K-edge peak indicates that Al, in general,

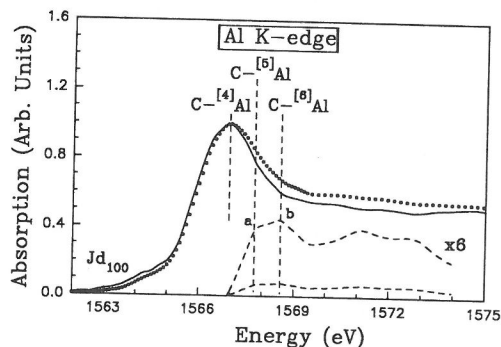


FIG. 4. Comparison of Al K-edge spectra of Jd_{100} glass (dot line) and crystalline albite (solid line). The $[4]Al$ K-edge peak is normalized to one unit in intensity, and the difference spectrum (dash line) between Jd_{100} glass and albite represents, in the immediate post-peak region, non- $[4]Al$ contributions to the glass spectrum.

is four-fold coordinated (Li *et al.*, 1995d). However, a weak shoulder at about 1568.5 eV appears in the Jd₆₀Ab₄₀ spectrum and becomes more evident in the Jd₁₀₀ spectrum (Fig. 4).

Figure 4 compares the Al K-edge spectra of the 4.4 GPa Jd₁₀₀ glass (dot line) and crystalline albite (solid line). Aluminum is four-fold coordinated in albite. Therefore, the difference spectrum (dash line) between the Jd₁₀₀ glass and crystalline albite represents some other contribution to the Jd₁₀₀ spectrum, in addition to ^[4]Al.

Figure 5 compares the difference spectra (dot lines) of Jd₁₀₀, Jd₈₀Ab₂₀ and Jd₆₀Ab₄₀ glasses, derived as in Fig. 4, with the Al K-edge spectra (solid lines) of crystalline corundum, containing ^[6]Al only, and crystalline andalusite, containing both ^[5]Al and ^[6]Al, as reference spectra (Li *et al.*, 1995d). The interval between adjacent data points in the region of the Al K-edge is 0.1 eV. Peaks a and b in the difference spectra of these glasses evidently correspond to the Al K-edge peaks of ^[5]Al and ^[6]Al, respectively (Li *et al.*, 1995d). Peak a is attributed to ^[5]Al and further assigned to transi-

tions of Al 1s electrons to antibonding ^[5]Al 3p-like states. Peak b is attributed to ^[6]Al and assigned to transitions of 1s electrons to antibonding ^[6]Al 3p-like t_{1u} states.

The Al K-edge XANES spectra of glasses along the Jd-Ab join indicate that at 4.4 GPa no or little ^[6]Al is present in Jd₂₀Ab₈₀ and Jd₄₀Ab₆₀ glasses, but ^[6]Al appears in Jd₆₀Ab₄₀ glass and becomes more evident with increasing Jd composition, to Jd₁₀₀ glass. These results also indicate that the pressure required for the four- to six-fold coordination change of Al in jadeite composition glass (*e.g.*, 4 GPa) is lower than that for albite glass quenched from the same temperature. The relative abundances of the different Al species in these glasses have been estimated from the relative intensity (simply represented by peak height) of the Al K-edge peak (Table 2). The abundances of both ^[5]Al and ^[6]Al species are estimated to be less than 1% in the Jd₂₀Ab₈₀ and Jd₄₀Ab₆₀ glasses, about 2.5% in the Jd₆₀Ab₄₀ glass, and increase to about 6% in the Jd₁₀₀ glass.

The temperature-pressure-composition conditions for which Al³⁺ may become six-fold coordinated in silicate melts have been debated among geochemists and geophysicists for some time. Computer simulation studies have suggested that pressures beyond 10 GPa may be required for the quantitative conversion of four- to six-fold coordinated Al (ANGELL *et al.*, 1982). HOCELLA and BROWN (1985) studied the structures of albite and jadeite composition glasses quenched from 1 and 1.5 GPa using X-ray scattering radial distribution functions, and reported no change in coordination of Al, observing only distortion of tetrahedral sites in the high-pressure materials. OHTANI *et al.* (1985) reported ^[6]Al in high-pressure glasses using ²⁷Al MAS NMR, but their results were not reproduced by STEBBINS and SYKES (1990). The present result of increasing ^[5]Al and ^[6]Al toward the Di end-member composition is consistent with the temperature-pressure-structure-composition relations along the NaAlSi₃O₈-SiO₂ join. However, the crystal-chemical control favoring ^[6]Al (and ^[5]Al) at the metasilicate (NaAlSi₂O₆) composition is not presently evident. The structure of high-pressure glasses beyond this composition (*i.e.*, along the NaAlSi₂O₆-NaAlSi₃O₈ join) is now of considerable interest.

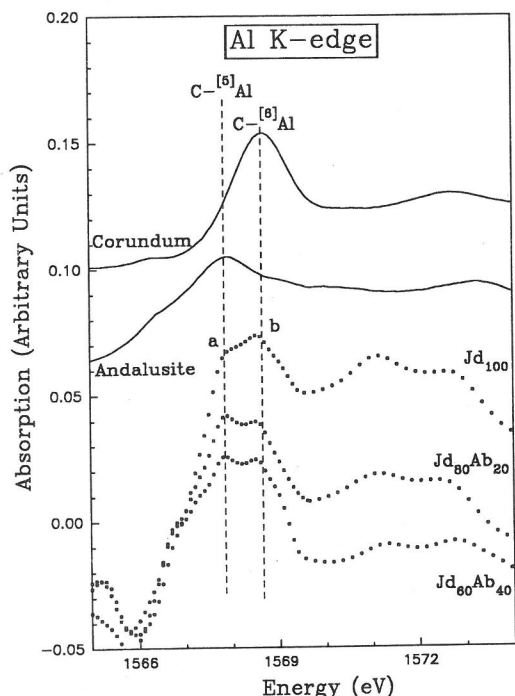


FIG. 5. The Al K-edge difference spectra of high-pressure glasses and crystalline albite (dot lines) compared with Al K-edge spectra (solid lines) of crystalline corundum (^[6]Al only) and andalusite (^[5]Al and ^[6]Al). Peaks a and b in the difference spectra of glasses correspond to the Al K-edge peak of ^[5]Al and ^[6]Al, respectively.

Si K-edge XANES spectra of Na₂Si₂O₅, Na₂Si₄O₉ and K₂Si₄O₉ glasses

Figure 6 shows the Si K-edge XANES spectra of the high-pressure phases ϵ -Na₂Si₂O₅ and wadeite-structure K₂Si₄O₉, and high-pressure glasses of composition Na₂Si₂O₅, Na₂Si₄O₉ and K₂Si₄O₉. The energy position of the Si K-edge peak indicates

Table 2. Abundances (%) of Al species in glasses along Jd-Ab join at 4.4 GPa

Sample	^[4] Al			^[5] Al			^[6] Al		
	Al K-edge*			Al K-edge*			Al K-edge*		
	Position	Height	Abundance	Position	Height	Abundance	Position	Height	Abundance
Jd ₁₀₀	1566.6	1.0	87.7	1567.7	0.066	5.8	1568.6	0.074	6.5
Jd ₈₀ Ab ₂₀	1566.6	1.0	92.4	1567.7	0.043	4.0	1568.5	0.040	3.6
Jd ₆₀ Ab ₄₀	1566.5	1.0	95.0	1567.7	0.026	2.5	1568.6	0.025	2.5
Jd ₄₀ Ab ₆₀	1566.5	1.0	~100.0	-	-	≤1.0	-	-	≤1.0
Jd ₈₀ Ab ₈₀	1566.5	1.0	~100.0	-	-	≤1.0	-	-	≤1.0
Andalusite				1567.8					
Corundum							1568.8		

* Errors for the position of Al K-edge are ± 0.1 eV; the height of Al K-edge is in arbitrary units. The errors for abundance values of ^[5]Al and ^[6]Al are $\pm 30\%$.

that Si is dominantly four-fold coordinated in the glasses. The post-edge features for the glasses are more or less washed out compared to those of the corresponding crystalline materials, as expected for the disordered structure of glasses. The Si K-edges of ϵ -Na₂Si₂O₅ (#1675) and the Na₂Si₂O₅ glasses are shifted to lower energy compared with vitreous Na₂Si₄O₉, in good agreement with the lower degree of polymerization of SiO₄ tetrahedra expected for the disilicate composition. The structure of epsilon sodium disilicate is based on a distorted disilicate sheet (Q³) of alternating six-membered rings of UUUDD and DDDDUU SiO₄ tetrahedra (FLEET and HENDERSON, 1995a). The slight upward shift in the Si K-edge of the disilicate glasses may reflect greater distortion of the disilicate rings at higher pressure. FLEET and HENDERSON (1995a) noted that ϵ -Na₂Si₂O₅ may be a model structure for the densification of silicate melts to moderate pressure, with densification accommodated dominantly by decrease in dihedral bond angle through crimping of ring structures.

In recent experiments with Na₂Si₂O₅ composition (FLEET and HENDERSON, work in progress), the ϵ -Na₂Si₂O₅ phase is stable to about 8.5 GPa, at which point it breaks down to Na₂Si₃O₇ (which has a novel structure with silicon in both 4- and 6-fold coordination and [⁶Si : ^[4]Si = 1 : 2]; FLEET and HENDERSON, 1995b), and an unidentified phase. Thus, ^[4]Si alone persists in the subsolidus to high pressure, and large amounts of ^[6]Si were not expected in the present sodium disilicate glasses. Similarly, sodium tetrasil-

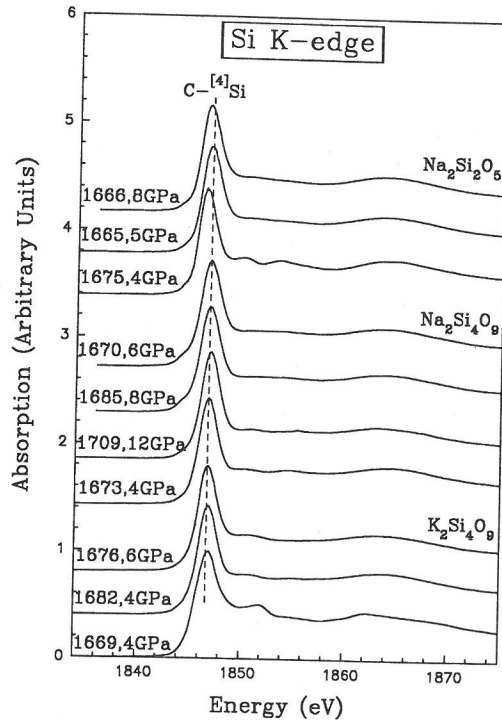


FIG. 6. Silicon K-edge XANES spectra of crystalline ϵ -Na₂Si₂O₅ (#1675), wadeite-structure K₂Si₄O₉ (#1669) and high-pressure Na₂Si₂O₅, Na₂Si₄O₉ and K₂Si₄O₉ glasses. The preparation conditions of the glasses are given in Table 1.

cate ($\text{Na}_6\text{Si}_3[\text{Si}_9\text{O}_{27}]$) (with $^{60}\text{Si} : ^{44}\text{Si} = 1 : 3$; FLEET, 1996) appears only above about 6 GPa. For example, experiment #1673 (Table 1, Fig. 6) yielded a product that was amorphous by optical examination, and this is confirmed by the suppressed post-edge features of its Si K-edge XANES spectrum. Therefore, we did not expect to see prominent features of ^{60}Si in the edge structures of the Si K-edge XANES spectra for the vitreous high-pressure sodium silicates. On the other hand, wadeite-structure $\text{K}_2\text{Si}_4\text{O}_9$ (#1669) is stable to much lower pressures (*e.g.*, SWANSON and PREWITT, 1983), no doubt because of the larger ionic radius of K^+ . A high energy shoulder is present at about 1849.0 eV in the Si K-edge spectrum of #1669, and represents the overlapped peak of C- ^{60}Si (LI *et al.*, 1994a). A similar shoulder is also present in the Si K-edge spectra of the two other high-pressure $\text{K}_2\text{Si}_4\text{O}_9$ glasses.

Figure 7 shows data reduction for the $\text{K}_2\text{Si}_4\text{O}_9$ glass quenched at 6 GPa (#1676). Fig. 7a compares the Si K-edge XANES spectra of the $\text{K}_2\text{Si}_4\text{O}_9$ glass (dot line) and room-pressure SiO_2 glass (solid line). The Si K-edge peak C- ^{44}Si of $\text{K}_2\text{Si}_4\text{O}_9$ glass and SiO_2 glasses are normalized to one unit in intensity. Because Si is all four-fold coordinated in room-pressure SiO_2 glass, the difference spectrum (dash line) between $\text{K}_2\text{Si}_4\text{O}_9$ glass and SiO_2 glass represents the contribution of ^{50}Si and/or ^{60}Si to the Si K-edge spectrum of the $\text{K}_2\text{Si}_4\text{O}_9$ glass. The Si K-edge spectra (dot lines) of ^{44}Si and ^{60}Si are curve-fitted into the corresponding Gaussian components (dash lines) in Figs. 7b and 7c, respectively, in which the solid curves are the envelopes of the fitted components and the backgrounds are included in the fitting procedures. Peak a is at about 1848.8 eV, very close to the typical position of C- ^{60}Si for crystalline materials containing six-fold coordinated Si at 1849.0 eV. Thus, peak a is attributed to ^{60}Si and assigned to transitions of Si 1s electrons to the antibonding 3p-like t_{1u} states (LI *et al.*, 1994a). The integrated areas of the ^{44}Si and ^{60}Si edge peaks are derived and used for the semi-quantitative estimation of abundance of ^{60}Si species (Table 3).

As noted above, crystalline $\text{K}_2\text{Si}_4\text{O}_9$ has the wadeite structure (SWANSON and PREWITT, 1983), for which $^{60}\text{Si} : ^{44}\text{Si} = 1 : 3$. Following the procedure in Fig. 7, the abundance of ^{60}Si in crystalline $\text{K}_2\text{Si}_4\text{O}_9$ is estimated to be about 22 % based on the integrated areas of ^{60}Si and ^{44}Si edge peaks, in good agreement with its X-ray crystal structure. The present analysis reveals little ^{60}Si is in $\text{Na}_2\text{Si}_2\text{O}_5$ composition glasses up to 8 GPa, and in $\text{Na}_2\text{Si}_4\text{O}_9$ composition glasses up to 8–12 GPa, as anticipated from the foregoing discussion. A trace of ^{60}Si is present in $\text{Na}_2\text{Si}_4\text{O}_9$ glass at 12 GPa. As expected, the $\text{K}_2\text{Si}_4\text{O}_9$ glasses

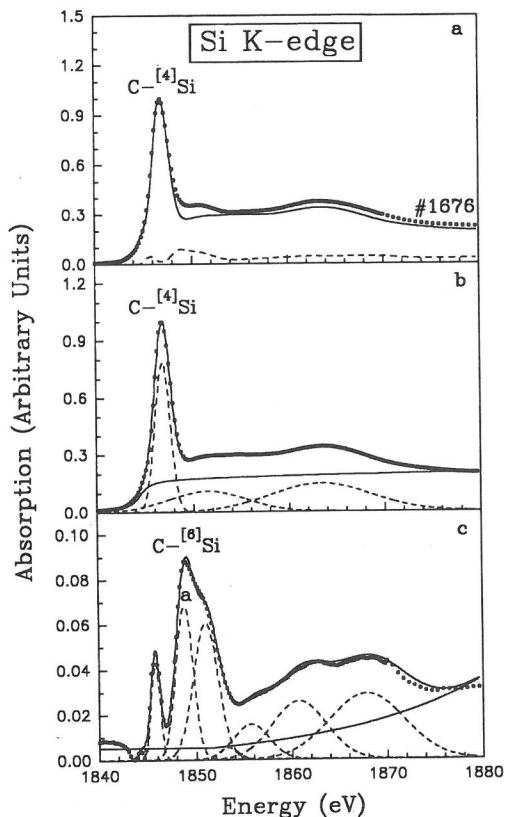


FIG. 7. Data reduction of the Si K-edge spectrum of the $\text{K}_2\text{Si}_4\text{O}_9$ glass (sample 1676) at 6 GPa. (a) Comparison of Si K-edge spectra of the $\text{K}_2\text{Si}_4\text{O}_9$ glass (dot line) and room-pressure SiO_2 glass (solid line), the dash curve is their corresponding difference spectrum. (b) Room-pressure SiO_2 glass spectrum (filled dot line) and (c) the difference spectrum (open dot line) are curve-fitted into the corresponding Gaussian components (dash lines). The solid curves are the corresponding envelopes of the fitted Gaussian components. The backgrounds are included in the fitting procedures.

have the highest abundance of ^{60}Si among the glasses investigated. For the present series of $\text{Na}_2\text{Si}_4\text{O}_9$ and $\text{K}_2\text{Si}_4\text{O}_9$ glasses, the abundance of ^{60}Si increases with increasing pressure, in good agreement with ^{29}Si MAS NMR spectroscopy (Table 3; XUE *et al.*, 1991). However, there are two principal discrepancies between the Si K-edge XANES and ^{29}Si MAS NMR measurements. First, little or no ^{50}Si is observed in the Si K-edge XANES spectra of the three series of glasses studied, but this may be because the ^{50}Si signal is too weak to be resolved in the Si K-edge spectra. Second, the ^{29}Si MAS NMR spectra showed a higher abundance of ^{60}Si in $\text{Na}_2\text{Si}_4\text{O}_9$ glasses than in $\text{K}_2\text{Si}_4\text{O}_9$ at the same pressure.

Table 3. Abundance of ^{69}Si in $\text{Na}_2\text{Si}_2\text{O}_5$, $\text{Na}_2\text{Si}_4\text{O}_9$, and $\text{K}_2\text{Si}_4\text{O}_9$ glasses, $\epsilon\text{-Na}_2\text{Si}_2\text{O}_5$ and wadeite-structure $\text{K}_2\text{Si}_4\text{O}_9$ from Si K-edge XANES and ^{29}Si MAS NMR

Sample	P (GPa)	^{41}Si edge (± 0.1 eV)	Si K-edge*		^{29}Si MAS NMR**	
			^{69}Si	^{67}Si	^{29}Si	^{31}Si
$\text{Na}_2\text{Si}_2\text{O}_5$						
1666	8	1846.6	≤ 1.0		1.5	~ 1.0
1665	5	1846.7	≤ 1.0		≤ 0.3	≤ 0.3
1675	4	1846.3	0.0			
$\text{Na}_2\text{Si}_4\text{O}_9$						
1709	12	1846.9	3.0		8.5	6.3
1685	8	1846.8	≤ 1.0		4.8	4.4
1670	6	1846.8	≤ 1.0		3.0	2.1
1673	4	1846.8	0.0			
$\text{K}_2\text{Si}_4\text{O}_9$						
1676	6	1846.9	8.9		3.9	1.5
1682	4	1846.8	5.0		1.5	0.2
1669	4	1846.9	22.0			

* Errors for the abundance values from Si K-edge XANES are $\pm 30\%$; ideal value is 0 for $\epsilon\text{-Na}_2\text{Si}_2\text{O}_5$ (#1675), and 25 for wadeite-structure $\text{K}_2\text{Si}_4\text{O}_9$ (#1669).

** The abundance values from ^{29}Si MAS NMR are cited in XUE *et al.* (1991).

Application of Si and Al K-edge XANES spectroscopy to study of glass structure

Silicon and Al K-edge XANES spectroscopy provide direct information on the nearest-neighbour coordination and intermediate-range structure in silicate and aluminosilicate glasses. The results to date are comparable to those of ^{29}Si and ^{27}Al MAS NMR spectroscopy, respectively, although detailed comparisons between these two techniques vary with the chemical element probed. ^{29}Si MAS NMR has superior resolution of spectral features compared with Si K-edge XANES, but Al K-edge XANES appears rather more useful than ^{27}Al MAS NMR. Also, XANES with synchrotron radiation requires only small (milligram) amounts of sample, and this is a distinct advantage for studying the products of high-pressure experiments.

The chemical and structural features revealed by Si and Al K-edge XANES collected by total electron yield (TEY) are not dominated by surface and near-surface contributions that are unrepresentative of the bulk glasses. Our experience to date is that Si K-edge XANES collected by TEY and fluorescence yield (FY) give comparable results. Fluorescence yield has appreciably greater sampling depth than TEY. This was elegantly demonstrated by KASRAI *et al.* (1996), who used films of amorphous SiO_2 of different thickness on silicon substrates to

determine sampling depths of 70 nm for Si K-edge XANES collected by TEY, and several hundred nm for comparable spectra collected by FY.

The pressure-induced changes in coordination of Si and Al presently reported are all close to the minimum detection limit of XANES spectroscopy. The estimated abundances of ^{69}Si in the alkali silicate glasses and of ^{51}Al and ^{69}Al in the $\text{NaAlSi}_3\text{O}_8$ - $\text{NaAlSi}_3\text{O}_8$ glasses are at best only semi-quantitative. Therefore, it is premature to attach too much significance to the discrepancies in abundance of ^{69}Si in the high-pressure alkali silicate glasses with the ^{29}Si MAS NMR study of XUE *et al.* (1991), although we have noted that the XANES results are more consistent with the stability of ^{69}Si in the subsolidus phases.

We also recognize that there is ambiguity in assigning specific structural features to shoulders on the edge peak of XANES spectra. However, the position of the edge peak is determined largely by the effective charge on the absorber atom (LI *et al.*, 1995a), which varies with nearest-neighbour coordination, degree of polymerization, network and network-modifying cation substitution, and so on. In silicate glasses, compression and distortion of TO_4 tetrahedral ring structures will be of subordinate importance, and are manifest largely by shift in position of the whole edge peak (rather than by

development of a shoulder), as well as change in FWHM.

In the absence of a quantitative unifying theory for XANES spectra, the use of labelled compounds is essential for their meaningful interpretation. We have used ϵ - $\text{Na}_2\text{Si}_2\text{O}_5$, wadeite-structure $\text{K}_2\text{Si}_4\text{O}_9$ and room-pressure SiO_2 glass to interpret the Si K-edge XANES spectra of the high-pressure alkali silicate glasses. Comparison of the Si K-edge XANES spectra of SiO_2 glass, quartz and stishovite (LI *et al.*, 1994a) with those of wadeite-structure $\text{K}_2\text{Si}_4\text{O}_9$ and the two high-pressure $\text{K}_2\text{Si}_4\text{O}_9$ glasses strongly supports the present structure assignments for the high-pressure alkali silicate glasses. The estimate of 22 % for the proportion of ^{16}Si in crystalline $\text{K}_2\text{Si}_4\text{O}_9$ (in good agreement with the ideal value of 25 %) was determined directly from the excess absorption of the edge peak after subtraction of the contribution due to ^{44}Si . Unfortunately, for the study of the high-pressure $\text{NaAlSi}_2\text{O}_6$ - $\text{NaAlSi}_3\text{O}_8$ glasses, we omitted to collect Al K-edge XANES spectra for the corresponding room-pressure glasses, and therefore used crystalline albite as the reference material.

Acknowledgements—We thank G. S. Henderson and J. A. Tossell for helpful reviews of the manuscript, H. Keppler for provision of $\text{CaMgSi}_2\text{O}_6$ - $\text{NaAlSi}_3\text{O}_8$ glass samples, R. A. Secco for synthesis of $\text{NaAlSi}_2\text{O}_6$ - $\text{NaAlSi}_3\text{O}_8$ glasses, Y. Thibault and R. W. Luth of C. M. Scarfe Laboratory of Experimental Petrology, University of Alberta, for running the experiments on $\text{Na}_2\text{Si}_2\text{O}_5$, $\text{Na}_2\text{Si}_4\text{O}_9$ and $\text{K}_2\text{Si}_4\text{O}_9$ samples, and M. Kasrai for assistance with graphics. We also acknowledge X. H. Feng at the Canadian Synchrotron Radiation Facility and staff at the Synchrotron Radiation Center (SRC), University of Wisconsin, for their technical assistance, and the National Science Foundation (NSF) for support of the SRC. This work was supported by the Natural Sciences and Engineering Research Council of Canada.

REFERENCES

- ANGELL C. A., CHEESEMAN P. A. and TAMADDON S. (1982) Pressure enhancement of ion mobility in liquid silicates from computer simulation studies to 800 kilobars. *Science* **218**, 885–887.
- DAVOLI I., PARIS E., STIZZA, S., BENFATO M., FANFONI M., GARGANO A., BIANCONI A. and SEIFERT F. (1992) Structure of densified vitreous silica: Silicon and oxygen XANES spectra and multiple scattering calculations. *Phys. Chem. Minerals* **19**, 171–175.
- DUPREE R., HOLLAND D. and MORTUZA M. G. (1987) Six-coordinated silicon in glasses. *Nature* **328**, 416–417.
- FARNAN I. and STEBBINS J. F. (1990) A high temperature ^{29}Si investigation of solid and molten silicates. *J. Amer. Chem. Soc.* **112**, 32–39.
- FINGER L. W. and HAZEN R. M. (1991) Crystal chemistry of six-coordinated silicon: a key to understanding the Earth's interior. *Acta Cryst.* **B47**, 561–580.
- FLEET M. E. (1996) Sodium tetrasilicate: A complex high-pressure framework silicate ($\text{Na}_6\text{Si}_3[\text{Si}_9\text{O}_{27}]$). *American Mineralogist*, in press.
- FLEET M. E. and HENDERSON G. S. (1995a) Epsilon sodium disilicate: A high pressure layer structure. *J. Solid State Chem.* **119**, 400–404.
- FLEET M. E. and HENDERSON G. S. (1995b) Sodium trisilicate: A new high-pressure silicate structure ($\text{Na}_2\text{Si}[\text{Si}_2\text{O}_7]$). *Phys. Chem. Minerals* **22**, 383–386.
- GALOISY L. and CALAS G. (1994) Network-forming Ni in silicate glasses. *Amer. Mineral.* **77**, 677–680.
- GIBBS J. H. and DIMARZIO E. A. (1958) Nature of the glass transition and the glassy state. *J. Chem. Phys.* **28**, 373–383.
- GREAVES G. N., FONTAINE A., LAGARDE P., RAOUS D. and GURMAN S. J. (1981) Local structure of silicate glasses. *Nature* **293**, 611–616.
- HEMLEY R. J., MAO H. K., BELL P. M. and MYSEN B. O. (1986) Raman spectroscopy of SiO_2 glass at high pressure. *Phys. Rev. Lett.* **57**, 747–750.
- HOCELLA M. F. and BROWN G. E. (1985) The structures of albite and jadeite composition glasses quenched from high pressure. *Geochim. Cosmochim. Acta* **49**, 1137–1142.
- ITO E. and TAKAHASHI T. (1987) Ultrahigh-pressure phase transformations and the reconstitution of the deep mantle. In *High-Pressure Research in Mineral Physics* (eds. M. H. MANGHNANI and Y. SYONO), *Geophys. Mono.* **39**, 221–229, American Geophysical Union, Washington D.C.
- JACKSON W. E., MUSTRE DE LEON J., BROWN G. E., WAYCHUNAS G. A., CONRADSON S. D. and COMBES J. M. (1993) High-temperature XAS study of Fe_2SiO_4 liquid: Reduced coordination of ferrous iron. *Science* **262**, 229–233.
- JEANLOZ R. (1990) The nature of the Earth's core. *Ann. Rev. Earth Planet. Sci.* **18**, 357–386.
- KASRAI M., LENNARD W. N., BRUNNER R. W., BANCROFT G. M., BARDWELL J. A. and TAN K. H. (1966) Sampling depth of total electron and fluorescence measurements in Si L- and K-edge absorption spectroscopy. *Appl. Surface Science*, submitted.
- KEPPLER H. (1992) Crystal field spectra and geochemistry of transition metal ions in silicate melts and glasses. *Amer. Mineral.* **77**, 62–77.
- KIRKPATRICK R. J. (1988) MAS NMR spectroscopy of minerals and glasses. In *Spectroscopic Methods in Mineralogy and Geochemistry* (ed. F. C. HAWTHORNE), *Rev. Mineral.* **18**, 341–403, Mineralogical Society of America, Washington D.C.
- KIRKPATRICK R. J., OESTRIKE R. and WEISS C. A. (1986) High-resolution ^{27}Al and ^{29}Si NMR spectroscopy of glasses and crystals along the join $\text{CaMgSi}_2\text{O}_6$ - $\text{CaAl}_2\text{SiO}_6$. *Amer. Mineral.* **71**, 705–711.
- LI DIEN, BANCROFT G. M., KASRAI M., FLEET M. E., SECCO R. A., FENG X. H., TAN K. H. and YANG B. X. (1994a) X-ray absorption spectroscopy of silicon dioxide (SiO_2) polymorphs: The structural characterization of opal. *Amer. Mineral.* **79**, 622–632.
- LI DIEN, BANCROFT G. M., KASRAI M., FLEET M. E., FENG X. H. and TAN, K. H. (1994b) High-resolution Si and P K- and L-edge XANES spectra of crystalline SiP_2O_7 and amorphous SiO_2 - P_2O_5 . *Amer. Mineral.* **79**, 785–788.
- LI DIEN, FLEET M. E., BANCROFT G. M., KASRAI M. and HENDERSON G. S. (1994c) Pressure-induced coordination change of Si in alkali silicate glasses by Si K-edge X-ray absorption spectroscopy (XAS). *EOS* **75**, 371.
- LI DIEN, BANCROFT G. M., FLEET M. E. and FENG

- X. H. (1995a) Silicon K-edge XANES spectra of silicate minerals. *Phys. Chem. Minerals.*, **22**, 115–122.
- LI DIEN, FLEET M. E., BANCROFT G. M., KASRAI M. and PAN Y. (1995b) Local structure of Si and P in $\text{SiO}_2\text{-P}_2\text{O}_5$ and $\text{Na}_2\text{O-SiO}_2\text{-P}_2\text{O}_5$ glasses: A XANES study. *J. Non-Cryst. Solids.*, **188**, 181–189.
- LI DIEN, BANCROFT G. M. and FLEET M. E. (1995c) Coordination of Si in $\text{Na}_2\text{O-SiO}_2\text{-P}_2\text{O}_5$ glasses using Si K- and L-edge XANES. *Amer. Mineral.*, in press.
- LI DIEN, BANCROFT G. M. and FLEET M. E. (1995d) Aluminum K-edge XANES spectra of aluminosilicate minerals. *Amer. Mineral.*, **80**, 432–440.
- LI DIEN, SECCO R. A., BANCROFT G. M. and FLEET M. E. (1995e) Pressure-induced coordination change of Al in silicate melts from Al K-edge XANES of high-pressure $\text{NaAlSi}_2\text{O}_6\text{-NaAlSi}_3\text{O}_8$ glasses. *Geophys. Res. Lett.*, in press.
- LIEBAU F. (1985) *Structural Chemistry of Silicates*. Springer-Verlag, Berlin.
- MCKEOWN, D. A., WAYCHUNAS, G. A. and BROWN G. E. (1985) EXAFS study of the coordination environment of aluminum in a series of silica-rich glasses and selected minerals within the $\text{Na}_2\text{O-Al}_2\text{O}_3\text{-SiO}_2$ system. *J. Non-Cryst. Solids* **74**, 349–371.
- MCMILLAN P. F. and PIRIOU B. (1983) Raman spectroscopic studies of silicate and related glass structure: A review. *Bull. Mineral.* **106**, 57–75.
- MCMILLAN P. F. (1984a) Structural studies of silicate glasses and melts — Applications and limitations of Raman spectroscopy. *Amer. Mineral.* **69**, 622–644.
- MCMILLAN P. F. (1984b) A Raman spectroscopic study of glasses in the system CaO-MgO-SiO_2 . *Amer. Mineral.* **69**, 645–659.
- MCMILLAN P. F., WOLF G. H. and POE B. T. (1992) Vibrational spectroscopy of silicate liquids and glasses. *Chem. Geol.* **96**, 351–366.
- MCMILLAN P. F., POE B. T., GILLET PH. and REYNARD B. (1994) A study of SiO_2 glass and supercooled liquid to 1950 K via high temperature Raman spectroscopy. *Geochim. Cosmochim. Acta* **58**, 3653–3664.
- MURDOCH J. B., STEBBINS J. F. and CARMICHAEL I. S. E. (1985) High-resolution ^{29}Si NMR study of silicate and aluminosilicate glasses. The effect of network-modifying cations. *Amer. Mineral.* **70**, 332–343.
- MYSEN B. O. (1988) *Structure and properties of silicate melts*. Elsevier, Amsterdam.
- MYSEN B. O. (1990) Role of Al in depolymerized, peralkaline aluminosilicate melts in the systems $\text{Li}_2\text{O-Al}_2\text{O}_3\text{-SiO}_2$, $\text{Na}_2\text{O-Al}_2\text{O}_3\text{-SiO}_2$, and $\text{K}_2\text{O-Al}_2\text{O}_3\text{-SiO}_2$. *Amer. Mineral.* **75**, 120–134.
- MYSEN B. O. (1995) Structural behavior of Al^{3+} in silicate melts: In situ, high-temperature measurements as a function of bulk chemical composition. *Geochim. Cosmochim. Acta* **59**, 455–474.
- MYSEN B. O. and FRANTZ J. D. (1993) Structure and properties of alkali silicate melts at magmatic temperatures. *Eur. J. Mineral.* **5**, 393–407.
- MYSEN B. O. and FRANTZ J. D. (1994) Structure of haplobasaltic liquids at magmatic temperature: In situ, high temperature study of melts on the join $\text{Na}_2\text{Si}_2\text{O}_5\text{-Na}_2 \times (\text{NaAl})_2\text{O}_5$. *Geochim. Cosmochim. Acta* **58**, 1711–1733.
- OHTANI E., TAULELLE F. and ANGELL, C. A. (1985) Al^{3+} coordination changes in liquid aluminosilicates under pressure. *Nature* **314**, 78–81.
- POE B. T., MCMILLAN P. F., COTE B., MASSIOT D. and COUTURES J. P. (1993) The Al environment in MgAl_2O_4 and CaAl_2O_4 liquids: An in situ study via high temperature NMR. *Science* **259**, 786–788.
- SEKIYA T., MOCHIDA N., OHTSUKA A. and UCHIDA K. (1988) 6-Coordinated Si^{4+} in $\text{SiO}_2\text{-PO}_{5/2}$ glasses — ^{29}Si MAS NMR method. *Nippon Seramikku Kyokai Gakujutsu Ronbunshi* **96**, 571–573.
- SMYTH J. R. and BISH D. L. (1988) *Crystal structures and cation sites of the rock-forming minerals*. Allen and Unwin, Boston.
- STEBBINS J. F. (1987) Identification of multiple structural species in silicate glasses by ^{29}Si NMR. *Nature* **330**, 465–467.
- STEBBINS J. F. (1988a) Effect of temperature and composition on silicate glass structure and dynamics: ^{29}Si NMR results. *J. Non-Cryst. Solids* **106**, 359–369.
- STEBBINS J. F. (1988b) NMR spectroscopy and dynamic process in mineralogy and geochemistry. In *Spectroscopic Methods in Mineralogy and Geochemistry* (ed. F. C. HAWTHORNE), *Rev. Mineral.* **18**, 405–429. Mineralogical Society of America, Washington D.C.
- STEBBINS J. F. (1991) NMR evidence for five-coordinated silicon in a silicate glass at atmospheric pressure. *Nature* **351**, 638–639.
- STEBBINS J. F. and FARNAN I. (1989) Nuclear magnetic resonance spectroscopy in the earth sciences: Structure and dynamics. *Science* **245**, 257–263.
- STEBBINS J. F. and MCMILLAN P. (1989) Five- and six-coordinated Si in $\text{K}_2\text{Si}_4\text{O}_9$ liquid at 1.9 GPa and 1200°C. *Amer. Mineral.* **74**, 965–968.
- STEBBINS J. F. and SYKES D. (1990) The structure of $\text{NaAlSi}_3\text{O}_8$ liquid at high pressure: new constraints from NMR spectroscopy. *Amer. Mineral.* **75**, 943–946.
- STOLPER E. M. and AHRENS T. J. (1987) On the nature of pressure-induced coordination changes in silicate melts and glasses. *Geophys. Res. Lett.* **14**, 1231–1233.
- SWANSON D. K. and PREWITT C. T. (1983) The crystal structure of $\text{K}_2\text{Si}^{14}\text{Si}_3\text{O}_9$. *Amer. Mineral.* **58**, 581–585.
- TAYLOR M. and BROWN G. E. (1979) Structure of silicate mineral glasses. I. The feldspar glasses $\text{NaAlSi}_3\text{O}_8$, KAlSi_3O_8 , $\text{CaAl}_2\text{Si}_2\text{O}_8$. *Geochim. Cosmochim. Acta* **43**, 1467–1473.
- WAYCHUNAS G. A., BROWN G. E., PONADER C. W. and JACKSON W. E. (1988) Evidence from X-ray absorption for network-forming Fe^{2+} in molten silicates. *Nature* **332**, 251–253.
- WILLIAMS Q. and JEANLOZ R. (1988) Spectroscopic evidence for pressure-induced coordination changes in silicate glasses and melts. *Science* **239**, 902–905.
- WONG J. and ANGELL C. A. (1976) *Glass Structure by Spectroscopy*. Marcel Dekker Inc., New York.
- XUE X., STEBBINS J. F., KANZAKI M. and TRØNNES R. G. (1989) Silicon coordination and speciation changes in a silicate liquid at high pressures. *Science* **245**, 962–964.
- XUE X., STEBBINS J. F., KANZAKI M., MCMILLAN P. F. and POE B. (1991) Pressure-induced silicon coordination and tetrahedral structural changes in alkali oxide-silica melts up to 12 GPa: NMR, Raman, and infrared spectroscopy. *Amer. Mineral.* **76**, 8–26.
- YANG B. X., MIDDLETON F. H., OLSSON B. G., BANCROFT G. M., CHEN J. M., SHAM T. K., TAN K. H. and WALLACE J. D. (1992) The design and performance of a soft X-ray double crystal monochromator beamline at Aladdin. *Nucl. Instr. Methods Phys. Res.* **A316**, 422–436.
- ZACHARIASEN W. H. (1932) The atomic arrangement in glass. *J. Amer. Chem. Soc.*, **54**, 3841–3851.

